Title:

Molecular prosthetics for long-term functional imaging with fluorescent reporters

Authors:

Vincent Grenier,[1*] Kayli N. Martinez,[1*] Brittany R. Benlian,[2*] Derek M. García-Almedina,[1*] Benjamin K. Raliski,[1] Steven C. Boggess,[1] Johnathan C. Maza,[1] Samantha J. Yang,[1] Evan W. Miller[1,2,3§]

Affliations:

[1]Department of Chemistry

[2]Deparment of Molecular & Cell Biology

[3]Helen Wills Neuroscience Institute

University of California, Berkeley, California, USA

94720-1460

Corresponding Author:

[§] evanwmiller@berkeley.edu

* Indicates equal contribution

Contact information:

VG: v.grenier@berkeley.edu, vgrenier@mr.mpg.de

KNM: kmarti11@berkeley.edu

BRB: brittanydaws@berkeley.edu

DMGA: derek.garcia@berkeley.edu

BKR: bkraliski@berkeley.edu

SCB: sboggess@berkeley.edu

JCM: jcmaza@berkeley.edu

SJY: samantha.yang@berkeley.edu

Main Text

Abstract

Voltage-sensitive fluorescent reporters can reveal fast changes in membrane potential in neurons and cardiomyocytes. However, in many cases, illumination in the presence of the fluorescent reporters results in disruptions to action potential shape that limits the length of recording sessions. We show here that a molecular prosthetic approach, previously limited to fluorophores, rather than indicators, can be used to substantially prolong imaging in neurons and cardiomyocytes.

Intro

Fluorophores are indispensable in the investigation of living systems. The problem is they bleach and can perturb the very system they are meant to observe. Bleaching makes it difficult to make sustained measurements, and phototoxicity introduces artifacts by disrupting the underlying physiology of the biological system. Exogenous photoprotectant cocktails, often containing anti-oxidants or triplet-state quenchers (TSQs), are often added to imaging media to prolong imaging duration by either reducing photobleaching or phototoxicity. Pioneering work showed that intramolecular tethering of a TSQ, like vitamin E derivative Trolox, or cyclooctatetrane (COT), profoundly improves the photostability and reduces phototoxicty of common fluorophores in single molecule[1] and cellular imaging.[2]

However, this self-healing fluorophore strategy has never been applied to fluorescent reporters: dyes which change their optical properties in response to biological cues, such as pH, Ca^{2+}, or membrane potential. Additionally, because the precise molecular mechanisms behind self-healing fluorophores remain under investigation,[3,4] it was not clear whether the presence of a TSQ would interfere with the sensing mechanism of the fluorescent reporter.

Voltage-sensitive dyes have often been limited by toxicity induced by the presence of dye and the intense illumination required for fast voltage imaging. We have been exploring new scaffolds for voltage imaging. While these dyes show decreased phototoxicity, because plasma membranes are especially sensitive to dye-sensitized photodamage,[5] we found that imaging of evoked neuronal action potentials under elevated illumination intensity (21 mW/mm^2) altered observed neuronal physiology, manifesting as non-evoked spikes, after-depolarizations, shifts in the baseline, and decreases in ΔF/F (**Figure S1**). We wondered whether the addition of exogenous photoprotectants, like Trolox or COT, might decrease the apparent disruptions to underlying neuronal physiology.

Background

To test this, we added Trolox or COT (1 mM) to see if this reduced the number of artifacts when imaging with mVF-sarcosine[6] (**Figure S1**) or with VF2.1.Cl (**Figure S6**).[7] Addition of Trolox has only a modest effect on the proportion of neurons that fire normally during field stimulation (27% ± 17%, 95% C.I.) compared to mVF-sarcosine alone (12% ± 11%), while COT significantly improves the fraction of normally firing neurons to 89% (± 10%) (**Figure S1**). However, application of millimolar concentrations of lipophilic photoprotectants is often not practical, and we wondered whether a covalently-tethered photoprotectant would reduce the impact on cellular physiology while retaining the voltage sensitivity of the native VF dye.

Synthesis

To test this hypothesis, we first synthesized a new VF dye, **1**, with a cysteic acid residue that possesses a sulfonic acid group for water solubility and retention in cell membranes, and a free amine, for ready

functionalization with Trolox or carboxy-COT (**Scheme S1**). From intermediate **1**, we synthesized a VF dye with covalently-tethered Trolox (**1**-Tro) or COT (**1**-COT) (**Figure 1a**).

In vitro and cellular characterization

The new VF-conjugates show absorption and emission nearly identical to the parent compound, with an absorbance maximum at 525 nm and an emission maximum near 540 nm (**Figure 1b**, **Figure S2**). In HEK293T cells, **1** is voltage sensitive, with a 18% ΔF/F per 100 mV (**Figure 1c**, **Figure S3**). Both the parent **1** and conjugates, **1**-Tro and **1**-COT, localize to cell membranes in HEK293T cells, neurons, and human induced pluripotent stem cell derived cardiomyocytes (hiPSC-CMs) (**Figure 1d-f**, **Figure S4**).

Imaging in neurons

We treated neurons with **1**-Tro, or **1**-COT and imaged optical action potentials driven by extracellular stimulation. We compared the results to imaging with **1** alone, or **1** plus the addition of exogenous photoprotective reagents Trolox or COT (**Figure 2a-b**). Similar to VF-sarcosine, imaging neuronal activity with **1** results in neurons without an artifact only 19% of the time (± 10%, 95% confidence interval). Neurons treated with Trolox (1 mM) showed no improvement, but imaging with Trolox covalently conjugated to **1** (500 nM, **1**-Tro) dramatically increased the proportion of neurons with artifact-free firing to 57% (± 16%). COT had an even more dramatic effect. When 1 mM exogenous COT was added to neurons loaded with **1**, the proportion of neurons without artifacts substantially increased, to 93% (± 8%). However, millimolar concentrations of COT—a 2000x excess over **1**—were required to observe this protective effect; at lower concentrations of 1 and 10 μM, still in stoichiometric excess over **1**, a high percentage of cells still displayed artifacts (**Figure S5**). When COT is covalently-attached to **1**, 96% of neurons fire normally (± 7%, **Figure 2b**).

Imaging in cardiomyocytes

Because of the excellent performance of **1**-COT in neurons, we investigated whether this protective effect could be observed in a distinct model system of electrically excitable cells. We loaded hiPSC-CMs with **1** alone (1 μM), **1** plus an equimolar amount of COT (1 μM), or the new **1**-COT conjugate (1 μM) (**Figure 2c-e**). The amplitude of cardiac action potentials (AP) drops dramatically during imaging with **1** alone (**Figure 2c**, black). Addition of equimolar COT helps maintain AP height; however, the signal to noise (SNR) is substantially degraded at the end of a 60 s imaging session (**Figure 2c**, blue). In contrast, AP height remains nearly constant throughout the 60 s imaging bout with **1**-COT (**Figure 2c**, green).

The protective effects of covalently-tethered COT are even more profound after periods of extended imaging. Even after 10 min of continuous illumination, the AP duration (APD) of hiPSC-CMs treated with **1**-COT remains unchanged (**Figure 2d**, green), while hi-PSC-CMs imaged with **1** alone show dramatic changes in APD even after 1 minute of illumination, significant changes to APD and shape after 5 minutes, and stop beating shortly thereafter (**Figure 2d**, black). Examination of AP shape during the initial 10 s of imaging (**Figure 2e**, t = 0) and after 5 minutes of continuous illumination reveal profound changes to the shape of APs in hiPSC-CMs imaged with **1**, while APs recorded after 5 min with **1**-COT overlay closely with initial APs (**Figure 2e**). Under maximum illumination, higher imaging speeds can be achieved using **1**-COT, enabling high temporal resolution recording of AP rise times and upstroke velocity (**Figure S7**).[8] Similar to the previously reported use of COT-conjugated fluorophores in live cells,[2] **1**-COT has a similar bleach rate to **1** (**Figure S8**), but substantially decreases phototoxicity.

Conclusion

In summary, we present a generalizable molecular prosthetic that can be used to stabilize recordings made with fluorescent reporters. Previous studies elegantly showed that covalent attachment of TSQs could prolong the duty cycle of fluorophores, but to date, no study has highlighted a similar strategy for fluorescent molecules that report dynamically on their environment. Here, we show specifically that covalent attachment of TSQs like Trolox or COT allow VF dyes to retain their performance in neurons or cardiomyocytes while avoiding disruptions to underlying cellular physiology. In contrast to previous studies in our lab, which altered the molecular wire of the voltage-sensitive fluorophore,[9,10] this present strategy has the potential to be more universal and could likely be applied to any VF dye (or other indicator), regardless of the molecular wire or fluorescent reporter.

Acknowledgments

EWM thanks the NIH (R35GM119855) and the Camille Dreyfus Teacher-Scholar Program for support of this research. KNM, BRB, DMGA, BKR, SCB, and JCM were supported, in part by the NIH (T32GM066698). VG was supported, in part, by NSERC.

Figures

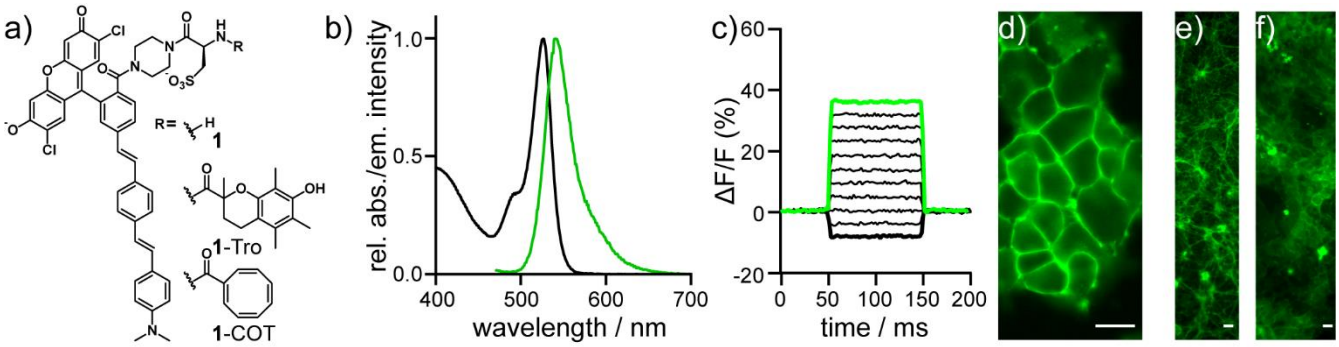

Figure 1. Characterization of TSQ-stabilized indicators. **a)** Structure of TSQ-stabilized Voltage-sensitive Fluorophores (VF dye). **b)** Plot of normalized absorbance and emission intensity for **1** (200 nM) in phosphate-buffered saline (PBS, pH 7.2) with 0.1% Triton X-100. **c)** Plot of relative change in fluorescence of **1** (ΔF/F) vs. time in a patch-clamped HEK293T cell under whole-cell voltage-clamp conditions. Widefield, epifluorescence images of **1**-COT in **d)** HEK293T cells (1 μM), **e)** cultured rat hippocampal neurons (0.5 μM), or **f)** hiPSC-derived cardiomyocytes (1 μM). All scale bars are 20 μm.

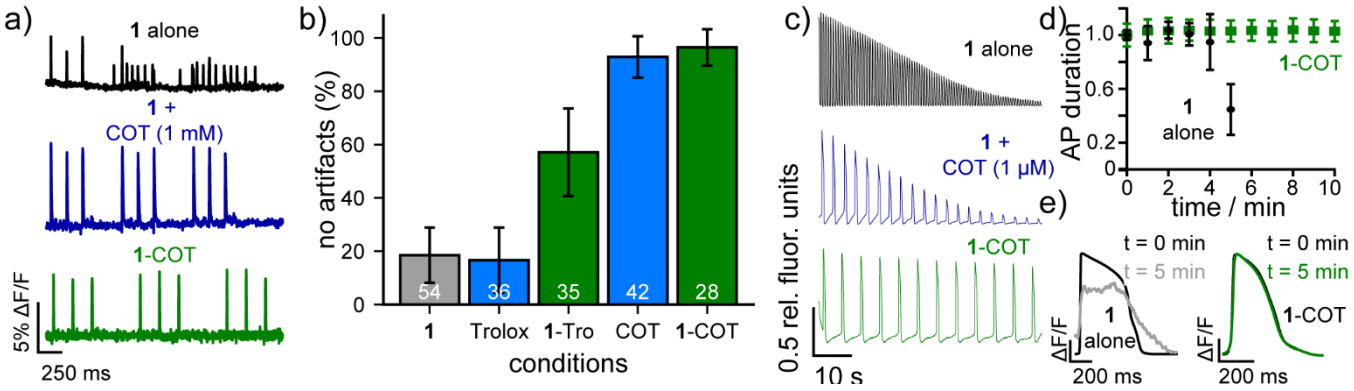

Figure 2. TSQ-stabilized indicators prevent unwanted physiological disruption in neurons and cardiomyocytes. **a)** Plots of relative fluorescence (ΔF/F) vs. time for neurons loaded with 500 nM of the indicated dye (**1**, black; **1** + 1 mM COT, blue; or **1**-COT, green) and stimulated with an extracellular electrode to evoke firing. Traces are single trials and are bleach corrected using a linear fit. **b)** Plot of fraction of neurons that exhibit no experimental artifacts during the neuronal simulation protocol, including shifts in baseline, after depolarizations, or non-evoked spikes. Data are the proportion of cells without artifacts. Error bars are 95% confidence interval. White values indicate the number of analyzed neurons per condition. **c)** Plot of relative fluorescence vs. time for unpaced hiPSC-CMs loaded with 1 μM of the indicated dye. Recordings are single trials and are bleach corrected using an asymmetric least squares fit. **d)** Plot of normalized action potential duration (APD) vs. time in spontaneously beating hiPSC-CMs loaded with **1** alone (black) or **1**-COT (green) and illuminated continuously for the indicated time. At 1 minute intervals, a 20 s movie was acquired and action potential shape was assessed. Data are mean ± S.E.M. for n = 3 separate experiments. **e)** Example optically-recorded action potentials for **1** alone (black/gray) or **1**-COT (black/green) at t = 0 min (black) and at t = 5 min (gray or green) of continuous illumination. AP traces are the average of 21 and 24 aligned APs for **1** alone (black/gray) and **1**-COT (black/green), respectively.

Supporting Information

Supporting Information for

Molecular prosthetics for long-term functional imaging with fluorescent reporters

Vincent Grenier,[1*] Kayli N. Martinez,[1*] Brittany R. Benlian,[2*] Derek M. García-Almedina,[1*] Benjamin K. Raliski,[1] Steven C. Boggess,[1] Johnathan C. Maza,[1] Samantha J. Yang,[1] Evan W. Miller[1,2,3§]

[1]Department of Chemistry

[2]Deparment of Molecular & Cell Biology

[3]Helen Wills Neuroscience Institute

University of California, Berkeley, California, USA

94720-1460

[§] evanwmiller@berkeley.edu

Synthetic Methods

Palladium catalysts and phosphine ligands were purchased from Strem Chemical. Deuterated solvents used for NMR studies were purchased from Cambridge Isotope Laboratories. Anhydrous solvents and all other chemical reagents were purchased from Sigma Aldrich, Acros Chemical, or Oakwood Chemical (South Carolina, USA) and used without further purification. References to previously synthesized compounds are provided along with characterization data. Thin layer chromatography (TLC) (Silicycle, F254, 250 μm) and preparative thin layer chromatography (PTLC) (Silicycle, F254, 1000 μm) were performed on glass backed plates pre-coated with silica gel and visualized by fluorescence quenching under UV light. Flash column chromatography was performed on Silicycle Silica Flash F60 (230–400 Mesh) using a forced flow of air at 0.5–1.0 bar. NMR spectra were measured on Bruker AVB-400 MHz, 100 MHz, AVQ-400 MHz, 100 MHz, Bruker AV-600 MHz, 150 MHz. Chemical shifts are expressed in parts per million (ppm) and are referenced to $CDCl_3$ (7.26 ppm, 77.0 ppm), DMSO-d_6 (2.50 ppm, 40 ppm), or acetone-d_6 (2.04 ppm, 29.8 and 206.3 ppm). Coupling constants are reported as Hertz (Hz). Splitting patterns are indicated as follows: s, singlet; d, doublet; t, triplet; q, quartet; dd, doublet of doublet; m, multiplet. High-resolution mass spectra (HR-ESI-MS) were measured by the QB3/Chemistry mass spectrometry service at University of California, Berkeley. High performance liquid chromatography (HPLC) and low resolution ESI Mass Spectrometry were performed on an Agilent Infinity 1200 analytical instrument coupled to an Advion CMS-L ESI mass spectrometer. The column used for the analytical HPLC was Phenomenex Luna 5 μm C18(2) (4.6 mm I.D. × 75 mm) with a flow rate of 1.0 mL/min. The mobile phases were MQ-H2O with 0.05% trifluoroacetic acid (eluent A) and HPLC grade acetonitrile with 0.05% trifluoroacetic acid (eluent B). Signals were monitored at 254, 350 and 480 nm over 10 min with a gradient of 10-100% eluent B unless otherwise noted. Ultra-high performance liquid chromatography (UHPLC) for purification of final compounds was performed using a Waters Acquity Autopurification system equipped with a Phenomenex Luna 10 μm C18(2) column (21.2 mm I.D. x 250 mm with a flow rate of 30.0 mL/min, made available by the Catalysis Facility of Lawrence Berkeley National Laboratory (Berkeley, CA)). The mobile phases were MQ-H2O with 0.05% trifluoroacetic acid (eluent A) and HPLC grade acetonitrile with 0.05% trifluoroacetic acid (eluent B). Signals were monitored at 254 and 350 nm over 20 min with a gradient of 10-100% eluent B, unless otherwise noted.

Steady-state UV-vis and fluorescence spectroscopy

Stock solutions of VoltageFluors were prepared in DMSO and diluted with PBS (10 mM KH_2PO_4, 30 mM $Na_2HPO_4 \cdot 7H_2O$, 1.55 M NaCl, pH 7.2) solution containing 0.10 % (w/w) SDS (1:500 dilution). UV-Vis absorbance and fluorescence spectra were recorded using a Shimadzu 2501 Spectrophotometer (Shimadzu) and a Quantmaster Master 4 L-format scanning spectrofluorometer (Photon Technologies International). The fluorometer is equipped with an LPS-220B 75-W xenon lamp and power supply, A-1010B lamp housing with integrated igniter, switchable 814 photon-counting/analog photomultiplier detection unit, and MD5020 motor driver. Samples were measured in 1-cm path length quartz cuvettes (Starna Cells).

Cell Culture

All animal procedures were approved by the UC Berkeley Animal Care and Use Committees and conformed to the NIH Guide for the Care and Use and Laboratory Animals and the Public Health Policy.

Human embryonic kidney cells (HEK293T)

HEK293T cells were acquired from the UC Berkeley Cell Culture Facility. Cells were passaged and plated onto 25 mm glass coverslips coated with Poly-D-Lysine (PDL; 1 mg/mL; Sigma-Aldrich) to a confluency of ~15% and 40% for electrophysiology and imaging, respectively. HEK293T cells were plated and

maintained in Dulbecco's modified eagle medium (DMEM) supplemented with 4.5 g/L D-glucose, 10% fetal bovine serum (FBS), and 1% Glutamax.

Rat hippocampal neurons

Hippocampi were dissected from embryonic day 18 Sprague Dawley rats (Charles River Laboratory) in cold sterile HBSS (zero Ca^{2+}, zero Mg^{2+}). All dissection products were supplied by Invitrogen, unless otherwise stated. Hippocampal tissue was treated with trypsin (2.5%) for 15 min at 37 °C. The tissue was triturated using fire polished Pasteur pipettes, in minimum essential media (MEM) supplemented with 5% fetal bovine serum (FBS; Thermo Scientific), 2% B-27, 2% 1M D-glucose (Fisher Scientific) and 1% glutamax. The dissociated cells were plated onto 12 mm diameter coverslips (Fisher Scientific) pre-treated with PDL (as above) at a density of 27,000 cells per coverslip in MEM supplemented media (as above). Neurons were maintained at 37 °C in a humidified incubator with 5 % CO_2. At 1 day in vitro (DIV) half of the MEM-supplemented media was removed and replaced with Neurobasal media containing 2% B-27 supplement and 1% glutamax.

Human induced pluripotent stem cell-derived cardiomyocytes (hiPSC-CMs)

hiPSCs (WTC11) were cultured on Matrigel (1:100 dilution; Corning)-coated 12 well-plates in StemFlex medium (Gibco). When the cell confluency reached 80–90%, which is referred to as day 0, the medium was switched to RPMI 1640 medium (Life Technologies) containing B27 minus insulin supplement (Life Technologies) and 10 µM CHIR99021 GSK3 inhibitor (Peprotech). At day 1, the medium was changed to RPMI 1640 medium containing B27 minus insulin supplement only. At day 3, medium was replaced to RPMI 1640 medium containing B27 supplement without insulin, and 5 µM IWP4 (Peprotech) for 2 days without medium change. On day 5, medium was replaced to RPMI 1640 medium containing B27 minus insulin supplement for 2 days without medium change. On day 7, medium was replaced with RPMI 1640 containing B27 with insulin supplement. After day 7, the medium was changed every two days. Confluent contracting sheets of beating cells appear between days 7 to 15.

Beating sheets were treated with collagenase II for 60-75 minutes. The collagenase solution was carefully transferred to cold DMEM, making sure cardiac sheets were not disturbed. Trypsin (0.25%) was added to dissociated sheets for 4-8 minutes and plated onto 6 well-plates coated with Matrigel (1:100 dilution) in RPMI 1640 medium containing B27 supplement plus ROCK inhibitor Y-27632. 24 hours later, the medium was replaced with fresh RMPI/B27 without ROCK inhibitor. Cardiomyocytes were maintained for 7 days, replacing media every other day, and then were switched to RPMI 1640 medium (-glucose) supplemented with 4 mM sodium lactate (Sigma Aldrich). Cells were maintained in this media for 7 days, replacing every other day, then switched back to RPMI/B27 containing glucose. These purified cardiomyocytes were then used for imaging.

Lactate purified sheets were dissociated with 0.25% trypsin-EDTA (4-8 minutes, depending on density and quality of tissue) and plated onto Matrigel (1:100)-coated Ibidi ® 24 well µ-plates (cat no. 82406) in RPMI 1640 medium containing B27 supplement (containing insulin). Medium was changed every 3 days until imaging. For loading hiPSC cardiomyocytes, voltage dyes were diluted 1 in 1000 in RPMI 1640 with B27 supplement minus Phenol Red to the desired final concentration. Cardiomyocytes were incubated in this solution for 20 minutes at 37 °C, then exchanged with dye-free RPMI 1640 with B27 supplement minus Phenol Red.

Fluorescence Imaging Conditions

For experiments with rat hippocampal neurons, Epifluorescence imaging was performed on an AxioExaminer Z-1 (Zeiss) equipped with a Spectra-X Light engine LED light (Lumencor), controlled with Slidebook (v6, Intelligent Imaging Innovations). Images were acquired with a W-Plan-Apo 20x/1.0 water objective (20x; Zeiss) and focused onto either an OrcaFlash4.0 sCMOS camera (sCMOS; Hamamatsu).

Inverted epifluorescence imaging of HEK293T cells and hiPSC cardiomyocytes was performed on an AxioObserver Z-1 (Zeiss), equipped with a Spectra-X Light engine LED light (Lumencor), controlled with µManager (V1.4, open-source, Open Imaging).[2,3] were acquired using a Plan-Apochromat 20/0.8 air objective (20x, Zeiss) or an EC-Plan-NEOFLUAR 40/1.3 oil immersion objective (40x; Zeiss). Images were focused onto an OrcaFlash4.0 sCMOS camera (sCMOS; Hamamatsu).

More detailed imaging information for each experimental application is expanded below.

Membrane staining in HEK293T cells

HEK293T cells were incubated with an imaging buffer (IB) solution (composition in mM: 139.5 NaCl, 10 HEPES, 5.6 D-glucose, 5.3 KCl, 1.3 $CaCl_2$, 0.49 $MgCl_2$, 0.44 KH_2PO_4, 0.41 $MgSO_4$, 0.34 Na_2HPO_4; 290 mOsm/kg, pH 7.25) containing VoltageFluors (500 nM) at 37 °C for 20 min prior to transfer to fresh IB (no dye) for imaging. Microscopic images were acquired with a 40X/1.3NA oil objective (Zeiss) and OrcaFlash4.0 sCMOS camera (Hamamatsu). For fluorescence images, the excitation light was delivered from a LED (9.5 mW/mm^2; 100 ms exposure time) at 475/34 (bandpass) nm and emission was collected with an emission filter (bandpass; 540/50 nm) after passing through a dichroic mirror (510 nm LP).

Voltage sensitivity in HEK293T cells

Functional imaging of the VoltageFluors was performed using a 40x/1.3 NA oil immersion objective paired with image capture from the sCMOS camera at a sampling rate of 0.5 kHz, focused onto a 100x100 pixel^2 ROI (binned 4x4, 66.5x66.5 µm^2). VoltageFluors were excited using the 475 nm LED with an intensity of 9.5 mW/mm^2. For initial voltage characterization, emission was collection with the emission filter and dichroic listed above.

Evoked activity in rat hippocampal neurons

Extracellular field stimulation was delivered by a SD9 Grass Stimulator connected to a recording chamber containing two platinum electrodes (Warner), with triggering provided through a Digidata 1440A digitizer and pCLAMP 10 software (Molecular Devices). Action potentials were triggered by 1 ms 80 V field potentials delivered at 5 Hz. To prevent recurrent activity the HBSS bath solution was supplemented with synaptic blockers 10 µM 2,3-Dioxo-6-nitro-1,2,3,4-tetrahydrobenzo[f]quinoxaline-7-sulfonamide (NBQX; Santa Cruz Biotechnology) and 25 µM DL-2-Amino-5-phosphonopentanoic acid (APV; Sigma-Aldrich). Functional imaging was performed using the sCMOS camera and a 20x water objective. VF dyes (500 nM in HBSS) were excited with a 475/34 (bandpass) nm LED with an intensity of 21 mW/mm^2 and emission was collected with an emission filter (bandpass; 540/50 nm) after passing through a dichroic mirror (510 nm LP).

Voltage recordings of hiPSC cardiomyocytes and assessment of phototoxicity

Functional recordings of voltage indicators (0.5 µM) were performed using a 20x air objective paired with a sCMOS camera at a sampling rate of 0.2 kHz (4x4 binning and restricted to a 512x125 pixel frame for high-speed acquisition over long periods). Indicators were excited at 475/34 (bandpass) nm with an intensity of 11.1 mW/mm^2 and emission was collected with an emission filter (bandpass; 540/50 nm) after passing through a dichroic mirror (510 nm LP). Routine recordings were made for ten seconds.

Phototoxicity of VoltageFluor dyes was assessed in cardiomyocyte monolayers incubated with 0.5 µM of indicator. These were exposed to constant illumination from the excitation LED (475/34; bandpass) for up to 14 minutes, while typical ten second fluorescence recordings were made at the beginning of each minute.

For upstroke velocity and rise time estimations (**Figure S7**), imaging experiments were performed as described above, but at maximum illumination intensity (25.4 mW/mm^2).

Image Analysis

HEK cell image analysis

Analysis of voltage sensitivity in HEK293T cells was performed using ImageJ (FIJI). Briefly, a region of interest (ROI) encompassing the cell body was selected and average fluorescence intensity was calculated for each frame. For background subtraction, a ROI encompassing a region without cells was selected and the average pixel intensity was calculated for each frame. A linear fit to the background trace was calculated and applied to the background, and this was used to subtract background signal from the fluorescence intensity trace. F/F_o values were calculated by dividing the background subtracted trace by the median value of fluorescence when the cell is held at -60 mV. ΔF/F values were calculated by plotting the change in fluorescence (ΔF) vs the applied voltage step and finding the slope of a linear best-fit.

Rat hippocampal neuron image analysis

For analysis of voltage responses in neurons, regions of interest encompassing cell bodies (all of approximately the same size) were drawn in ImageJ and the mean fluorescence intensity for each frame extracted. ΔF/F values were calculated by first subtracting a mean background value from all raw fluorescence frames to give a background subtracted trace. A least squares linear regression was fit to the background subtracted trace and a bleaching curve, derived from the slope of the regression, was used to correct for photobleaching. A baseline fluorescence value (Fbase) was calculated from the median of all the frames and was subtracted from each timepoint of the bleach corrected trace to yield a ΔF trace. The ΔF was then divided by Fbase to give ΔF/F traces. No averaging was applied to any voltage traces.

Traces were then scored for the presence of artifacts (see **Figure S1c-g** for examples), including non-evoked spikes, after-depolarizations, and shifts in the baseline. Scoring of neurons was performed by 3 different experimenters. Experimenters were blind to the experimental conditions during scoring. The proportion of responding cells for each dye/condition was noted, and 95% confidence intervals were constructed according to the **Equation S1**.

$$\mathrm{C.I.} = z^* \sqrt{\frac{p(1-p)}{n}} \qquad \textbf{Equation S1}$$

Where C.I. is the confidence interval, p is the proportion of cells that show no artifacts during the trial, n is the number of cells analyzed, and z* is critical value of z at 95% confidence (z* = 1.96 for 95% confidence interval).

hiPSC-CM image analysis

Analysis of action potential (AP) data from hiPSC cardiomyocytes was performed using in-house MATLAB scripts based on previously developed software by the Efimov lab (Washington University, St. Louis, MO). Scripts are available upon request. Briefly, raw OME-tiffs recorded in μManager was read directly into MATLAB for batch-processing of large datasets (>30 Gb per experiment). The mean pixel intensity of the entire image (512x125 pixels) was calculated for each frame and a mean fluorescence trace was extracted for the entire stack. Photobleach correction was performed by subtracting an asymmetric least-squares fit of the data from the mean trace. No subtraction of background was possible due to staining of the entire monolayer. Individual AP events were identified through threshold detection based on a Schmidtt trigger. Action potential duration (APD) values were calculated for each AP by finding the activation time (time of the maximum derivative of the AP upstroke) and the time the signal returns to

70, 50, and 10% of the maximum depolarization (APD30, APD50, APD90, respectively). APD values were corrected for variation due to spontaneous beat rate by Fridericia's formula (**Equation S2**). CL is the cycle length, calculated as the time period from the beginning of one beat to the beginning of the succeeding beat.

$$\mathrm{APDc} = \frac{APD}{\sqrt[3]{CL}} \qquad \textbf{Equation S2}$$

Electrophysiology

For electrophysiological experiments in HEK293T, pipettes were pulled from borosilicate glass with filament (Sutter Instruments, BF150-86-10) with a P-97 pipette puller (Sutter Instruments) to a resistance of 4-7 MΩ. Pipettes were filled with an internal solution (composition, in mM): 125 potassium gluconate, 10 HEPES, 10 KCl, 5 NaCl, 2 ATP disodium salt, 1 EGTA, 0.3 GTP sodium salt (pH 7.25, 285 mOsm). Pipettes were positioned with an MP-225 micromanipulator (Sutter Instruments). Electrophysiological recordings were obtained with an Axopatch 200B amplifier (Molecular Devices) at room temperature. The signals were digitized with a Digidata 1440A , sampled at 50 kHz, filtered at 5 kHz and recorded with pCLAMP 10 software (Molecular Devices).

Electrophysiology was performed in the whole cell voltage clamp configuration. After gigaseal formation and break-in, recordings were only pursued if series resistance in voltage clamp was less than 30 MΩ and the recording maintained a 30:1 ratio of membrane resistance to access resistance throughout all voltage steps. No series resistance compensation was applied. Fast capacitance was compensated in the cell attached configuration. All voltage clamp protocols were corrected for the calculated liquid junction (-14 mV, Liquid Junction Potential Calculator in pClamp). For tandem electrophysiology and fluorescence intensity recordings, cells were held at -60 mV and de- and hyper- polarizing steps were applied from +100 to -100 mV in 20 mV increments, with each step lasting 100 ms.

Supporting Figures

Figure S1. VF-sarcosine + photoprotectants

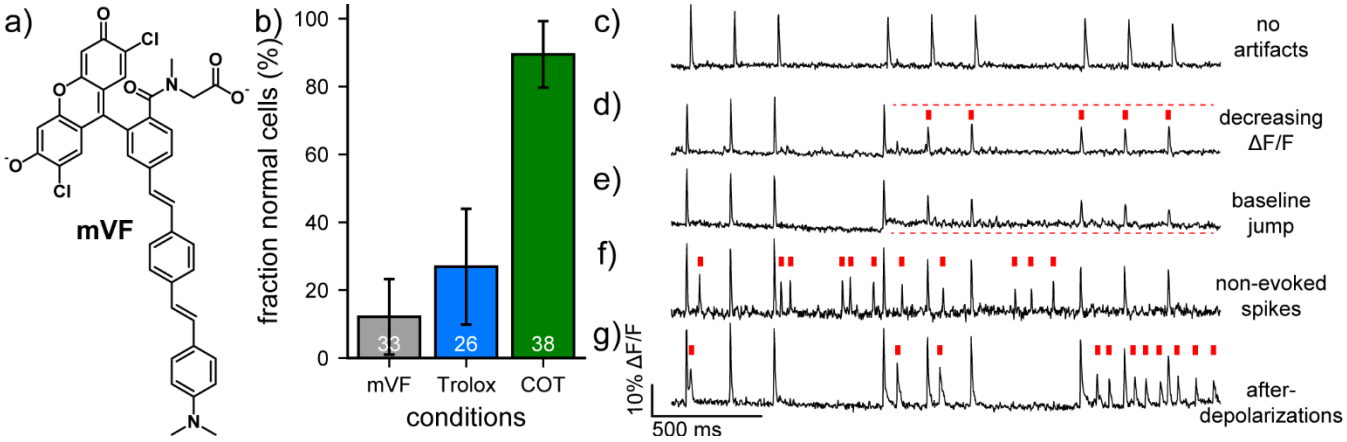

Figure S1. Effect of exogenous photoprotectants on neuronal activity imaging with mVF-sarcosine. **a)** Structure of mV used in these experiments (compound **13** from Grenier, *et al. JACS*, **2019**, *141*, 1359). **b)** Plot of fraction of normally-firing neurons (i.e. no shifts in baseline, after depolarization, or non-evoked spikes) vs. condition for rat hippocampal neurons imaged with **mVF** (500 nM) and subjected to the evoked activity protocol. Trolox and cyclooctatetraene (COT) were applied at a concentration of 1 mM. Error bars are the 95% confidence interval for each proportion. The number of neurons analyzed for each condition is indicated in white at the base of the bars. **c-g)** Example plots of neuronal activity traces used to determine normal firing. All plots are plots of fractional change in fluorescence (ΔF/F) in rat hippocampal neurons stained with 500 nM mVF-sarc and stimulated with 3 sets of 3 pulses to evoke action potentials (APs). **c)** An example of a recording with no artifacts—this cell fires normally. **d)** An example of decreasing ΔF/F in the 2nd and 3rd round of stimulation. The dotted red line indicates the approximate ΔF/F for APs in the first round of recording. Red bars indicate APs with lower ΔF/F. **e)** An example of a baseline jump. The dotted red line during the 2nd round of stimulation shows the off-set increase in baseline fluorescence. **f)** An example of a recording with non-evoked spikes. Red bars indicate spikes that arrived regardless of stimulation. **g)** An example of after-depolarizations, in which additional spikes are recorded after the stimulated spike. Red bars indicate after-depolarizations.

Figure S2. **Absorption and Emission**

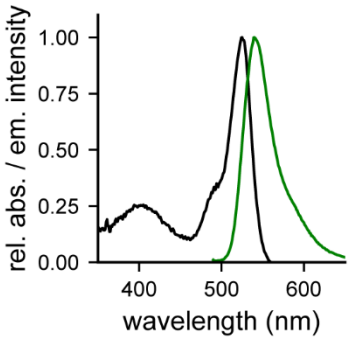

Figure S2. Absorption and emission spectra of **1**-COT. Plots of normalized absorbance and emission intensity for **1**-COT (200 nM) in phosphate-buffered saline (PBS, pH 7.2) with 0.1% Triton X-100.

Figure S3. Voltage sensitivity of 1 (plot of ΔF/F vs mV)

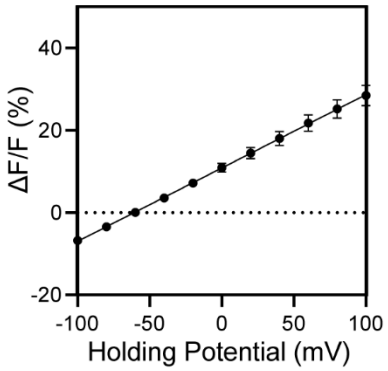

Figure S3. Voltage sensitivity of **1**. Plot of fractional change in fluorescence (ΔF/F) vs. membrane potential for **1**. Data are mean ± standard error of the mean for n = 9 determinations. Voltage sensitivity is 18% ± 0.6% (S.E.M.)

Figure S4. Images of compounds in HEK cells, neurons, and hiPSC-CMs

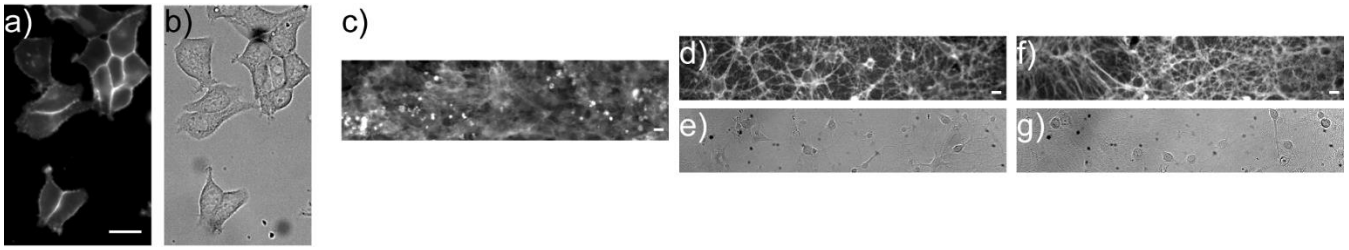

Figure S4. Imaging of **1** or **1**-Tro in HEK293T cells, neurons, and hiPSC-CMs. **a)** Widefield epifluorescence and **b)** transmitted light images of **1** in HEK cells. Widefield epifluorescence image of **1** in **c)** hiPSC-CMs, or **d)** dissociated rat hippocampal neurons. **e)** Transmitted light image of panel **d**. **f)** Widefield epifluorescence and **g)** transmitted light images of **1-Tro** in dissociated rat hippocampal neurons. Scale bars are 20 μm for all images.

Figure S5. COT titration in neurons

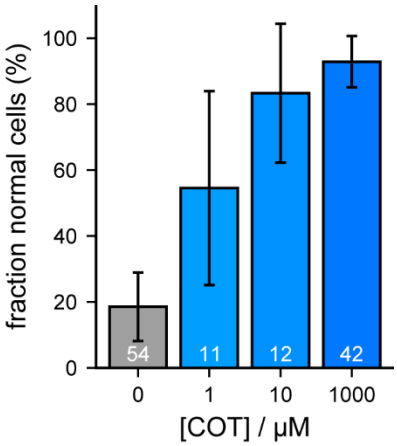

Figure S5. Titration of cylcooctatetraene (COT) in neurons. Plot of fraction of normally-firing neurons (i.e. no shifts in baseline, after depolarization, non-evoked spikes, or after-depolarizations) vs. concentration of COT (in μM) for rat hippocampal neurons imaged with **1** and subjected to the evoked activity protocol. Error bars are the 95% confidence interval for each proportion. The number of neurons analyzed for each condition is indicated in white at the base of the bars. Data for 0 μM and 1,000 μM COT are repeated from the main text, **Figure 2**, for ease of comparison.

Figure S6. **Comparison of all dyes andconditions in neurons**

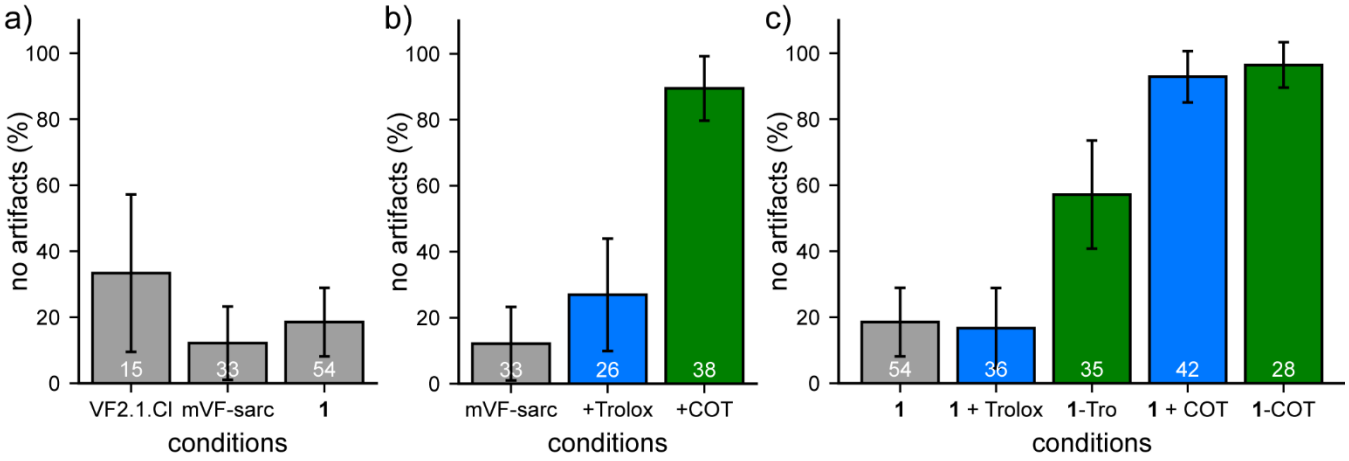

Figure S6. Comparison of all dyes and conditions in neurons. Plots of fraction of normally-firing neurons (i.e. no shifts in baseline, after depolarization, non-evoked spikes, or after-depolarizations) vs. all analyzed dye and additive conditions. **a)** Plot of normally-firing neurons vs. VF dye with no additives. VF2.1.Cl, mVF-sarc, or Compound **1**. Data for mVF-sarc and **1** are repeated from **Figure S1b** and **Figure 2b**, respectively, for comparison). **b)** Plot of normally-firing neurons vs. mVF-sarc with addition of exogenous Trolox (1 mM) and COT (1 mM). Data are repeated from **Figure S1b** for ease of comparison. **c)** Plot of normally-firing neurons vs. **1**, **1** + Trolox (1 mM), **1**-Tro, **1** + COT (1 mM), or **1**-COT. Data are repeated from **Figure 2b** in the main text, for ease of comparison. All error bars are ± 95% confidence interval. Numbers of neurons analyzed are indicated in white at the base of the respective bar.

Figure S7. Action potential kinetics estimation under high-speed, high-powered illumination

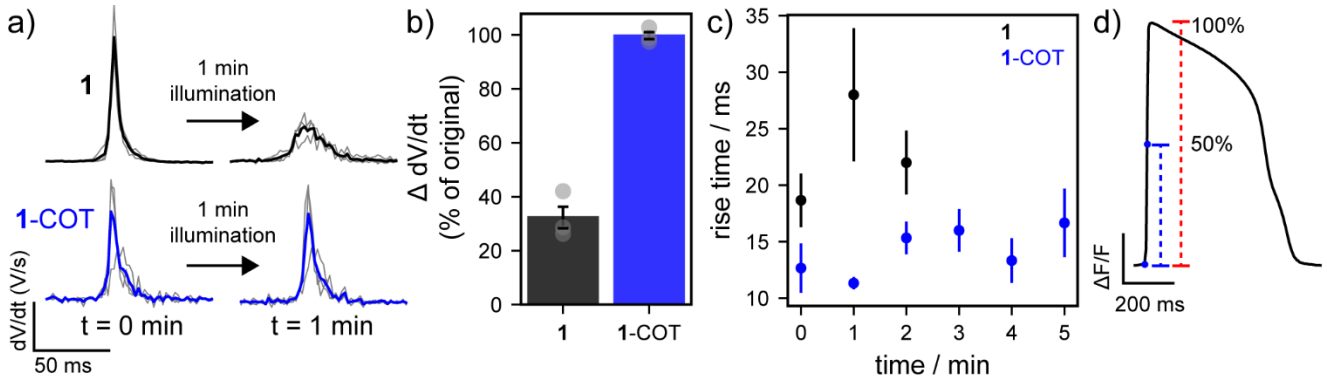

Figure S7. Action potential kinetics estimation under high-speed, high-powered illumination. **a)** Plots of maximum upstroke velocity (dV/dt, in units of V/s) vs. time for action potentials (AP) recorded with either **1** (black traces) or **1**-COT (blue traces). Thick colored line (black or blue) are the mean dV/dt values, individual dV/dt plots are in grey (n = 3 independent experiments). Plots show t = 0 min of illumination and after 1 min of continuous illumination. The mean dV/dt value was calculated by estimating an AP amplitude of 100 mV (Table 1 in *Front. Physiol.* **2012**, *3*, 346; mean AP amplitude = 100 mV). Across all 6 experiments, including APs recorded with both **1** and **1**-COT, the mean upstroke velocity is 11.4 V/s (±3.2 V/s, standard deviation, n = 6), which is within the range of recorded upstroke velocities for hiPSC-CMs reported in Hoekstra, *et al.* (Table 1 in *Front. Physiol.* **2012**, *3*, 346; mean dV/dt = 31 V/s, min = 9 V/s, max = 115 V/s).[8] **b)** Plot of the change in dV/dt (ΔdV/dt) as a percentage of original dV/dt after one minute of high powered illumination for **1** alone (black) or **1**-COT (blue). Data are mean ΔdV/dt; error bars are S.E.M. for n = 3, and individual differences (paired before/after) are in grey circles. **c)** Plot of rise time vs. total illumination time for **1** (black) and **1**-COT (blue). Data are mean rise time (in ms); error bars are S.E.M. for n = 3 independent experiments. **d)** Rise times are calculated as the time difference between the initial rise from baseline (first blue circle) to the maximum slope at 50% (second blue dot, or blue dashed line) of maximum AP height (red dotted line). A schematized AP from **Figure 2e** in the main text is shown for illustrative purposes.

Figure S8. Photobleaching comparison in hiPSC-CMs

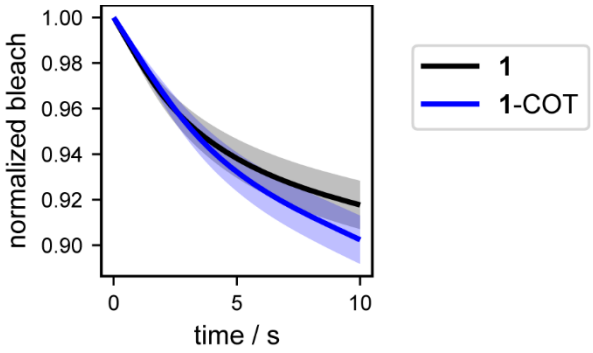

Figure S8. Photobleaching comparison in hiPSC-CMs. Plot of normalized photobleach rate for **1** or **1**-COT vs. time in hiPSC-CMs. Data are mean bleach rate for **1** (black line) or **1**-COT (blue line). Shaded area represents 95% confidence interval for n = 5 independent determinations.

Table S1. Summary of neuron imaging data

Dye	additive	[additive]	no artifacts (#)	no artifacts (%)	total cells	Figure
1	---	---	10	19%	54	2b / S6c
1	Trolox	1 mM	6	17%	35	2b / S6c
1	COT	1 mM	39	93%	42	2b / S6c
1-Tro	---	---	20	57%	35	2b / S6c
1-COT	---	---	27	96%	28	2b / S6c
1	COT	0.001 mM	6	55%	11	S5
1	COT	0.01 mM	10	83%	12	S5
mVF-sarc[a]	---	---	4	12%	33	S1b / S6b
mVF-sarc[a]	Trolox	1 mM	7	27%	26	S1b / S6b
mVF-sarc[a]	COT	1 mM	34	89%	38	S1b / S6b
VF2.1.Cl[b]	---	---	5	33%	15	S6a

[a] Compound **13** from Grenier, *et al. JACS*, **2019**, *141*, 1359. [b] VF2.1.Cl from Miller, *et al. PNAS*, **2012**, *109*, 2114.

Scheme S1. Synthesis of 1, 1-Tro, and 1-COT

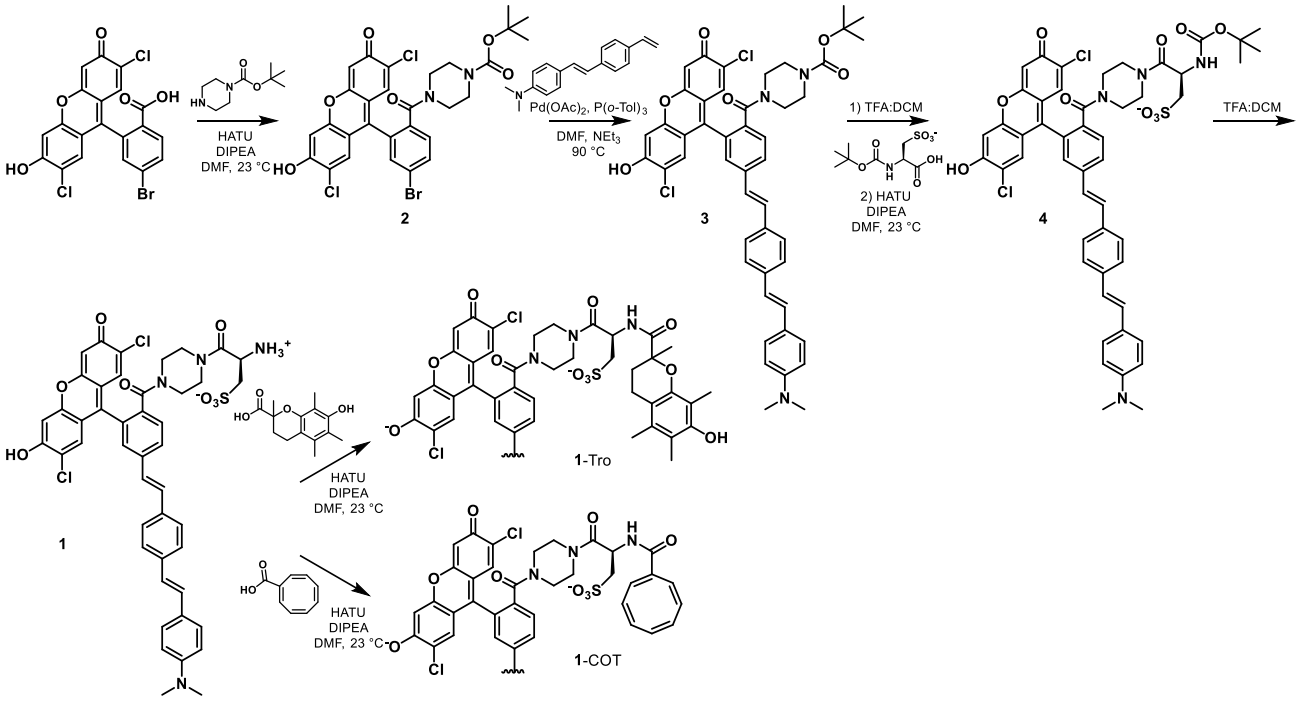

Synthesis of **2**.

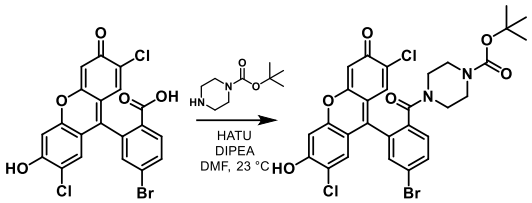

2

Synthesis of **2**, or, *tert*-butyl 4-(4-bromo-2-(2,7-dichloro-6-hydroxy-3-oxo-3*H*-xanthen-9-yl)benzoyl)piperazine-1-carboxylate.

6-bromo-2',7' dichlorofluorescein (317 mg, 660 µmol), Boc-protected piperazine (127.6 mg, 685 µmol) and HATU (695 µmol) were dissolved in 2 mL anhydrous DMF, followed by addition of 575 µL DIPEA (427 mg, 3.30 mmol). After stirring for 24 hours the reaction was diluted with 50 mL 20% iPrOH/DCM and washed five times with 20 mL water. The organic phase was dried over MgSO4, decanted, and solvents removed under reduced pressure. Product was purified by flash column chromatography (10% MeOH/DCM) to obtain **2** (380 mg, 586 µmol, 89%) as a red powder. Analytical HPLC retention time: 6.89 minutes.

^{1}H NMR (300 MHz, d_6-DMSO) δ 7.95 (dd, *J* = 8.3, 2.1 Hz, 1H), 7.85 (d, *J* = 2.0 Hz, 1H), 7.62 (d, *J* = 8.3 Hz, 1H), 7.17 (s, 2H), 6.77 (s, 2H), 3.38 (bm, 4H), 3.13 (bm, 4H)1.4 (s, 9H).

ESI-MS: $[M+H]^+$ calculated 647.0, found 647.2.

$[M-C_3H_8+H]^+$, calculated 591.0, found 591.1

Spectra S1. HPLC of 2.

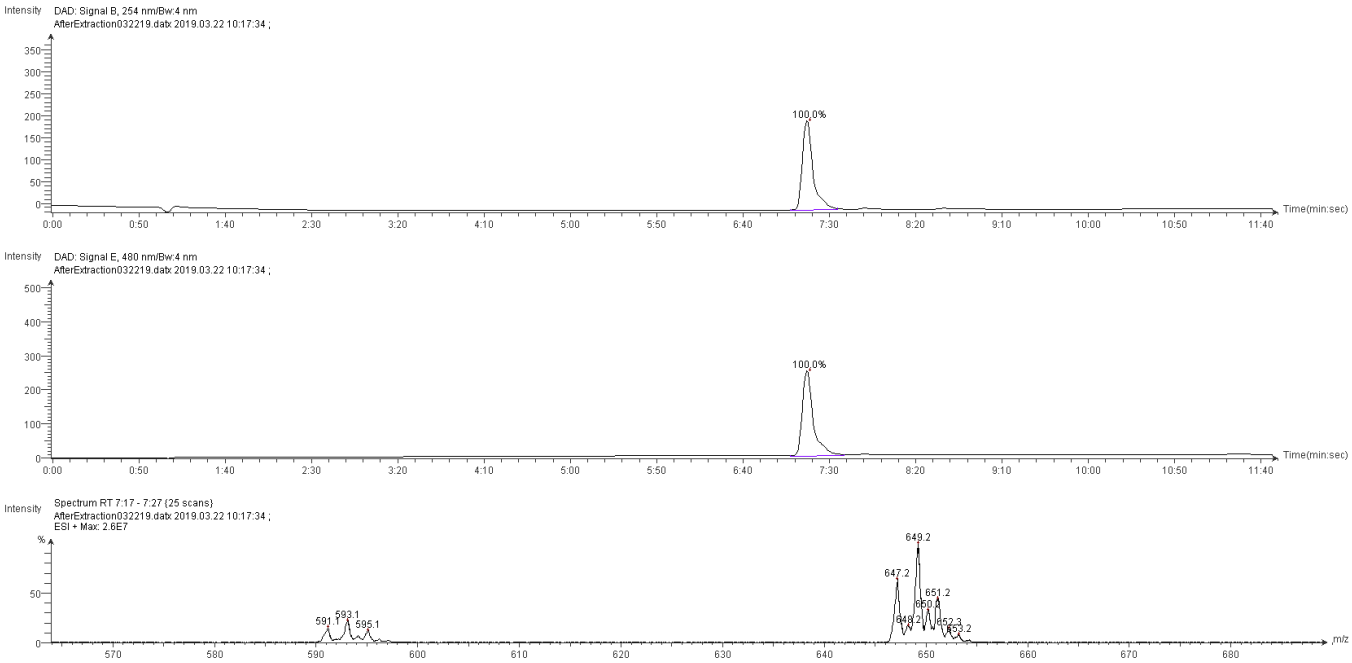

Synthesis of **3**.

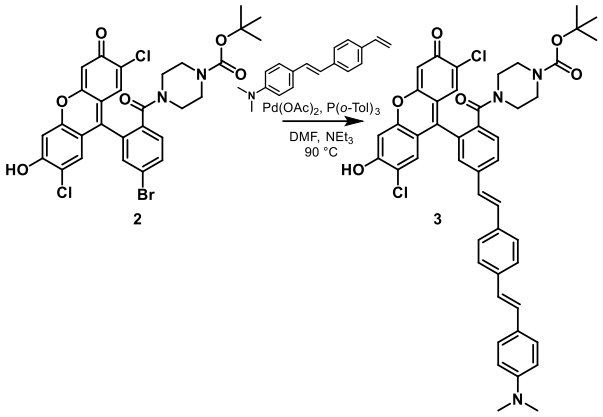

Synthesis of **3**, or, tert-butyl 4-(2-(2,7-dichloro-6-hydroxy-3-oxo-3*H*-xanthen-9-yl)-4-((*E*)-4-((*E*)-4-(dimethylamino)styryl)styryl)benzoyl)piperazine-1-carboxylate.

To an oven-dried Schlenk flask added **2** (350 mg, 540 µmol), phenylene vinylene molecular wire (169 mg, 678 µmol), $Pd(OAc)_2$ (1.80 mg, 8.01 µmol) and P(*o*-Tol)$_3$ (15.5 µmol). The flask was evacuated and backfilled with N_2 three times. Solid reagents were dissolved in 3 mL anhydrous DMF, 1.5 mL anhydrous Et3N and the reaction stirred for 16 hours at 90 °C. After cooling to rt the reaction was diluted with 20 mL 20% iPrOH/DCM and filtered through a pad of celite. Solvents were removed under reduced pressure and product purified by flash column chromatography (10% MeOH/DCM) to obtain **3** (408 mg, 500 µmol, 92%) as a red powder.

^{1}H NMR (300 MHz, d_6-DMSO) δ 7.91 (d, *J* = 2.1 Hz, 1H), 7.82 (d, *J* = 1.9 Hz, 1H), 7.76 (s, 1H), 7.65 (d, *J* = 8.1 Hz, 1H), 7.61-7.48 (m, 4H), 7.47-7.43 (m, 3H), 7.15 (d, *J* = 3.0 Hz, 3H), 7.00 (s, 1H), 6.72 (m, 4H), 3.12 (m, 8H), 2.93 (s, 6H), 1.40 (s, 9H).

ESI-MS $[M+H]^+$ calculated 816.3 , found 816.4.

Spectra S2. HPLC of 3

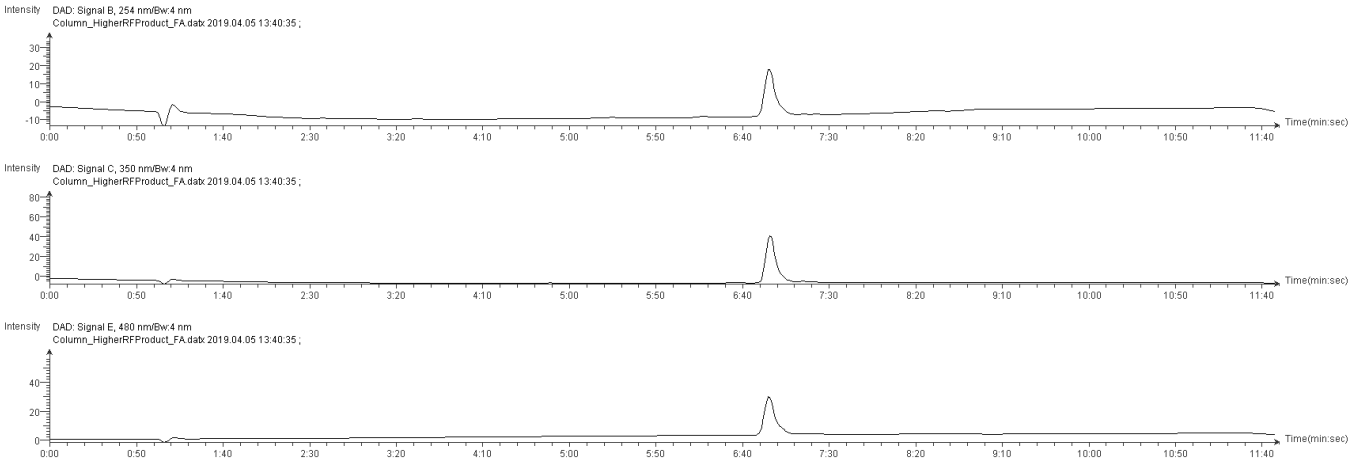

Synthesis of **4**.

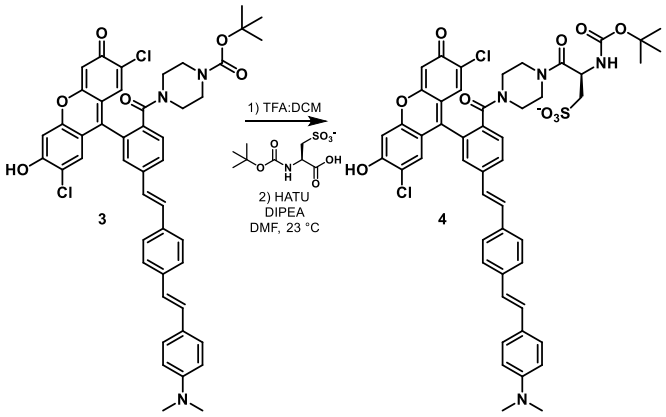

Synthesis of **4**, or (*R*)-2-((tert-butoxycarbonyl)amino)-3-(4-(2-(2,7-dichloro-6-hydroxy-3-oxo-3*H*-xanthen-9-yl)-4-((*E*)-4-((*E*)-4-(dimethylamino)styryl)styryl)benzoyl)piperazin-1-yl)-3-oxopropane-1-sulfonate

3 (154.3 mg, 188 µmol) was dissolved in 2 mL 1:1 TFA:DCM. After stirring for 30 minutes the reaction was concentrated under a stream of N_2 and residual solvents removed by toluene azeotrope. In the same round bottom, added Boc-protected cysteic acid (56.0 mg, 208 µmol) and HATU (82.5 mg, 217 µmol). Solid reagents were dissolved in 1 mL anhydrous DMF, followed by addition of 164 µL DIPEA (121 mg, 164 µmol). After stirring for 16 hours the reaction was neutralized by drop-wise addition of AcOH and solvents removed under reduced pressure. Crude material was purified by preparative TLC (15% MeOH, 5% AcOH in DCM, material eluted off silica with 10% MeOH/DCM) to obtain **4** as a red gum. Trituration with MeCN led to formation of a red powder, which could be isolated by vacuum filtration to obtain **4** (90.0 mg, 93.0 µmol, 50%).

ESI-MS [M+H]+ calculated 967.3 , found 967.5.

Spectra S3. HPLC of 4

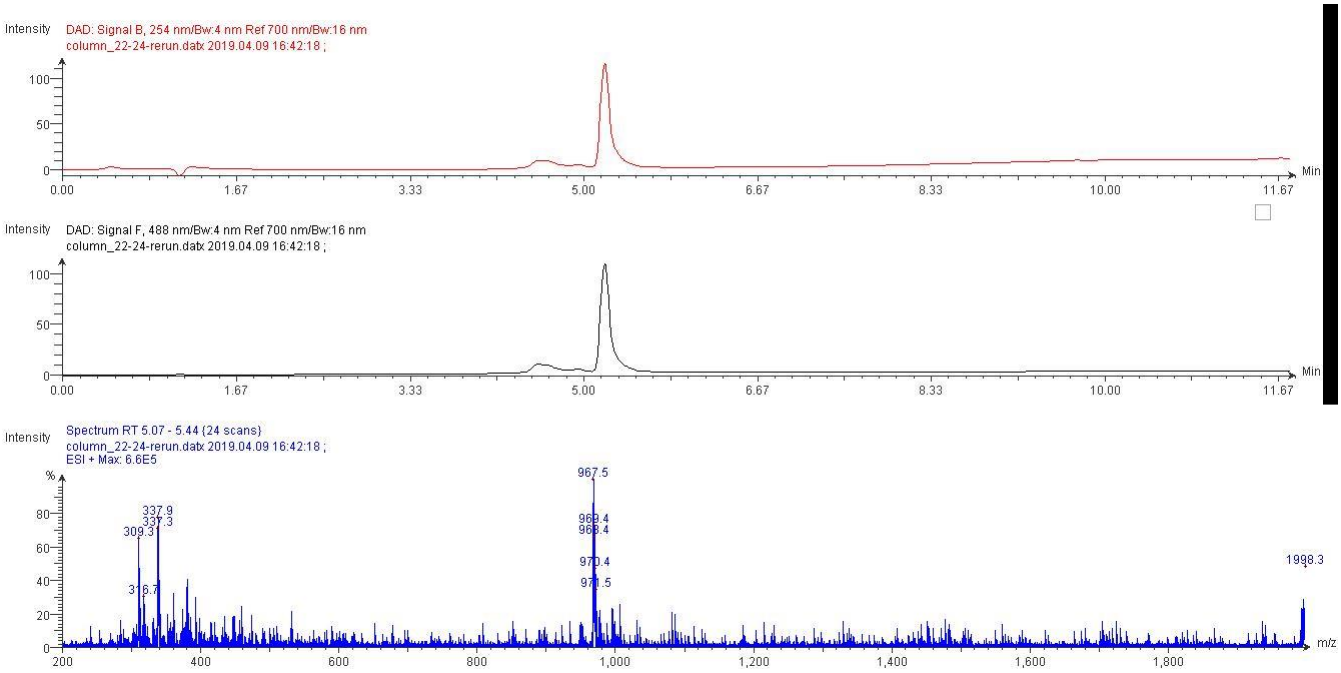

Synthesis of **1**.

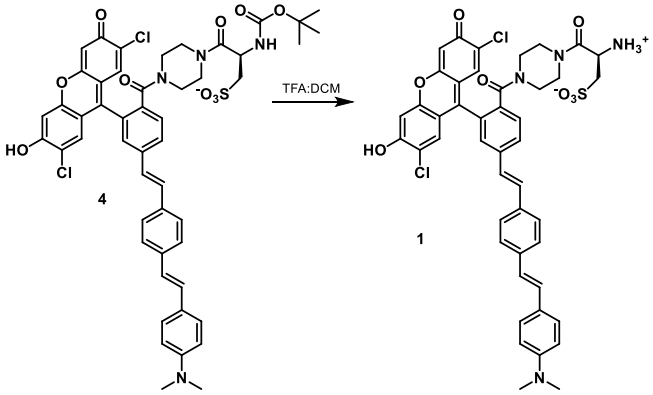

Synthesis of **1**, or, (*R*)-2-ammonio-3-(4-(2-(2,7-dichloro-6-hydroxy-3-oxo-3*H*-xanthen-9-yl)-4-((*E*)-4-((*E*)-4-(dimethylamino)styryl)styryl)benzoyl)piperazin-1-yl)-3-oxopropane-1-sulfonate.

4 (47.9 mg, 51.7 μmol) was dissolved in 1 mL 1:1 TFA:DCM. After stirring for 30 minutes, the reaction was concentrated under a stream of N_2, after which residual solvents were removed by toluene azeotrope under reduced pressure. The resulting solid was suspended in MeCN and **1** (40.1 mg, 37.3 μmol, 90%) was collected by vacuum filtration as an orange powder. Analytical HPLC retention time: 4.67 minutes.

^{1}H NMR (600 MHz, d_6-DMSO) δ 8.03 (s, 3H), 7.93 (d, *J* = 8.2 Hz, 1H), 7.77 (s, 1H), 7.68 (d, *J* = 8.1 Hz, 1H), 7.61 – 7.50 (m, 3H), 7.50 – 7.30 (m, 4H), 7.18 (d, *J* = 16.3 Hz, 2H), 6.98 (d, *J* = 16.3 Hz, 1H), 6.73 (d, *J* = 8.5 Hz, 2H), 4.47 (s, 1H), 3.66 – 3.54 (m, 6H), 3.17 – 3.06 (m, 2H), 2.94 (s, 6H).

ESI-MS $[M+H]^+$ calculated 867.2 , found 867.2.

Spectra S4. HPLC of 1

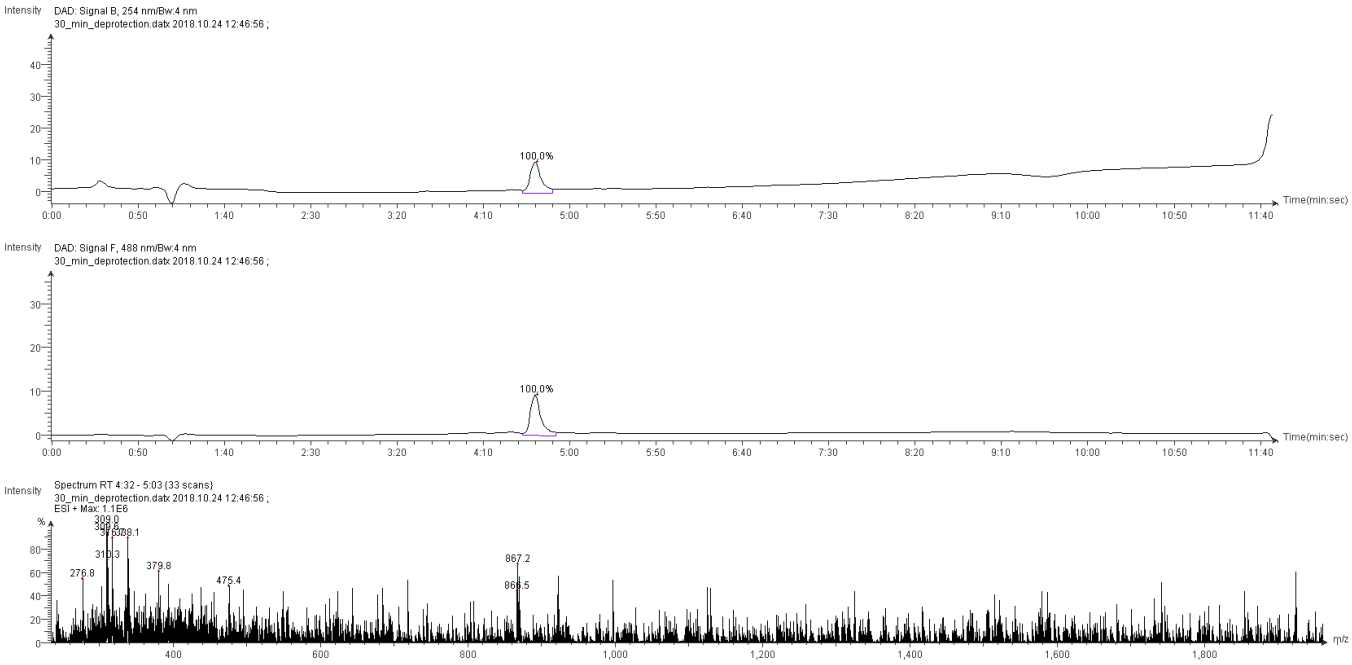

Synthesis of **1**-Tro.

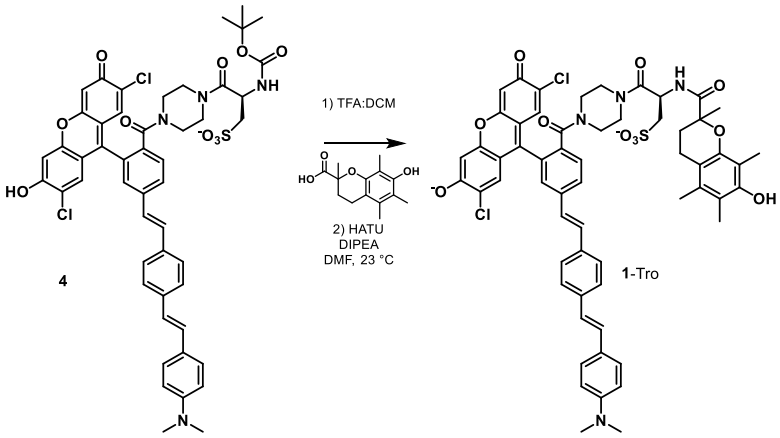

Synthesis of **1**-Tro, or, (2*R*)-3-(4-(2-(2,7-dichloro-6-oxido-3-oxo-3*H*-xanthen-9-yl)-4-((*E*)-4-((*E*)-4-(dimethylamino)styryl)styryl)benzoyl)piperazin-1-yl)-2-(7-hydroxy-2,5,6,8-tetramethylchromane-2-carboxamido)-3-oxopropane-1-sulfonate

4 (42.1 mg, 43.5 μmol) was dissolved in 1 mL 1:1 TFA:DCM. After stirring for 1 hour the reaction was concentrated under a stream of N_2 and residual solvents removed by toluene azeotrope. In the same round bottom, added Trolox (12.2 mg, 48.6 μmol) and HATU (19.1 mg, 50.1 μmol). Solid reagents were dissolved in 1 mL anhydrous DMF, followed by addition of 37.9 μL DIPEA (28.1 mg, 217 μmol). After stirring for 16 hours the reaction was neutralized by addition of 50 μL AcOH and solvents removed under reduced pressure. The crude reaction was dissolved in MeOH, filtered through a 0.22 μm filter and purified by preparative HPLC to obtain **1**-Tro (9.49 mg, 8.63 μmol, 20%) as an orange powder.

^{1}H NMR (600 MHz, d_6-DMSO) δ 7.93 (d, *J* = 8.3 Hz, 1H), 7.75 (s, 1H), 7.67 (dd, *J* = 8.1, 4.9 Hz, 1H), 7.57 (m, 4H), 7.51-7.31 (m, 4H), 7.17 (m, 3H), 7.00 (d, *J* = 16.3 Hz, 1H), 6.79 (m, 3H), 5.76 (s, 1H), 4.70 (m, 2H), 3.41 (s, 4H), 3.13-3.04 (m, 1H), 2.95 (s, 6H), 2.80-2.57 (m, 3H), 2.06 (m, 7H), 1.98 (m, 3H), 1.75-1.62 (m, 1H).

ESI-MS $[M+H]^+$ calculated 1099.3, found 1099.5.

Spectra S5. HPLC 1-Tro

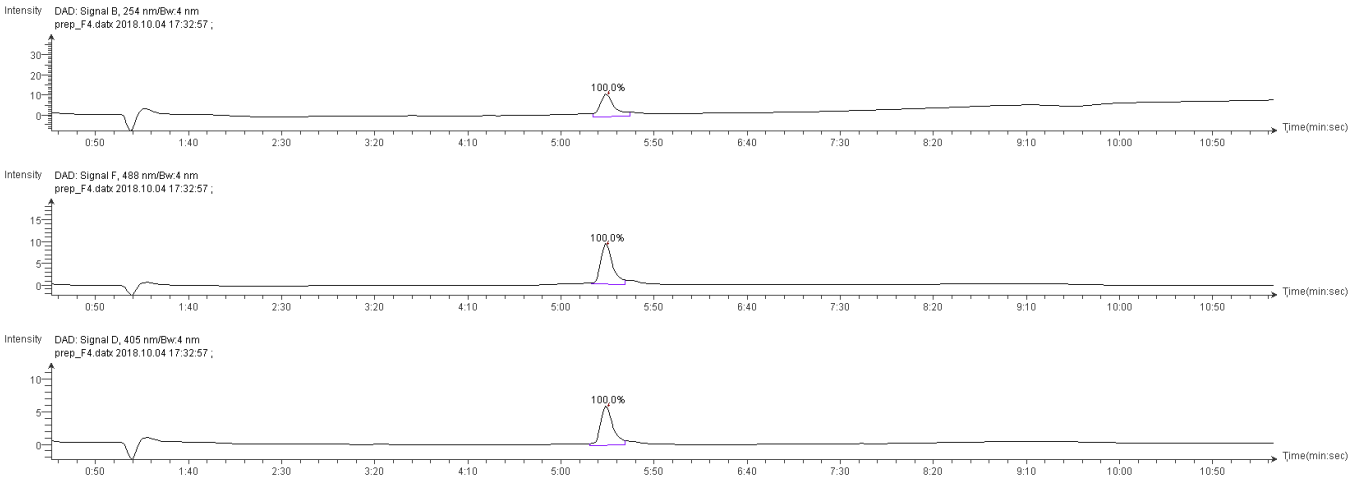

Synthesis of **1**-COT.

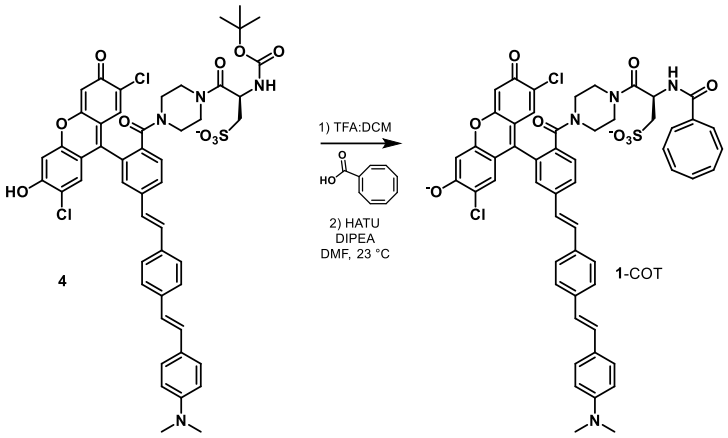

Synthesis of **1**-COT, or, (*R*)-2-((1*E*,3*Z*,5*Z*,7*Z*)-cycloocta-1,3,5,7-tetraene-1-carboxamido)-3-(4-(2-(2,7-dichloro-6-oxido-3-oxo-3*H*-xanthen-9-yl)-4-((*E*)-4-((*E*)-4-(dimethylamino)styryl)styryl)benzoyl)piperazin-1-yl)-3-oxopropane-1-sulfonate.

From DMGA summary (only source):

4 (23.6 mg, 24.4 µmol) was dissolved in 1 mL 1:1 TFA:DCM. After stirring for 30 minutes the reaction was concentrated under a stream of N_2, after which residual solvents were removed by toluene azeotrope. To the same reaction vial, added COT-CO_2H (8.6 mg, 58.1 µmol) and HATU (18.4 mg, 48.4 µmol). Solid reagents were dissolved in 0.25 mL anhydrous DMF, followed by addition of 0.03 mL DIPEA (22.3 mg, 172 µmol). After stirring for 16 hours, the reaction was neutralized by drop-wise addition of AcOH and solvents removed under reduced pressure, azeotroping with toluene. Crude material was purified by preparative TLC (15% MeOH, 5% AcOH in DCM, material eluted off silica with 10% MeOH/DCM) to obtain **1**-COT as a red gum (>95% pure by HPLC). Azeotroping with toluene led to formation of a red powder (14.5 mg, 60%).

ESI-MS $[M+H]^+$ calculated 997.2 , found 997.3.

High resolution ESI-MS $[M-H]^-$ calculated 995.2290 ($^{12}C_{54}H_{45}O_9N_4{}^{35}Cl_2{}^{32}S_1$), found 995.2292.

Spectra S6. HPLC of 1-COT

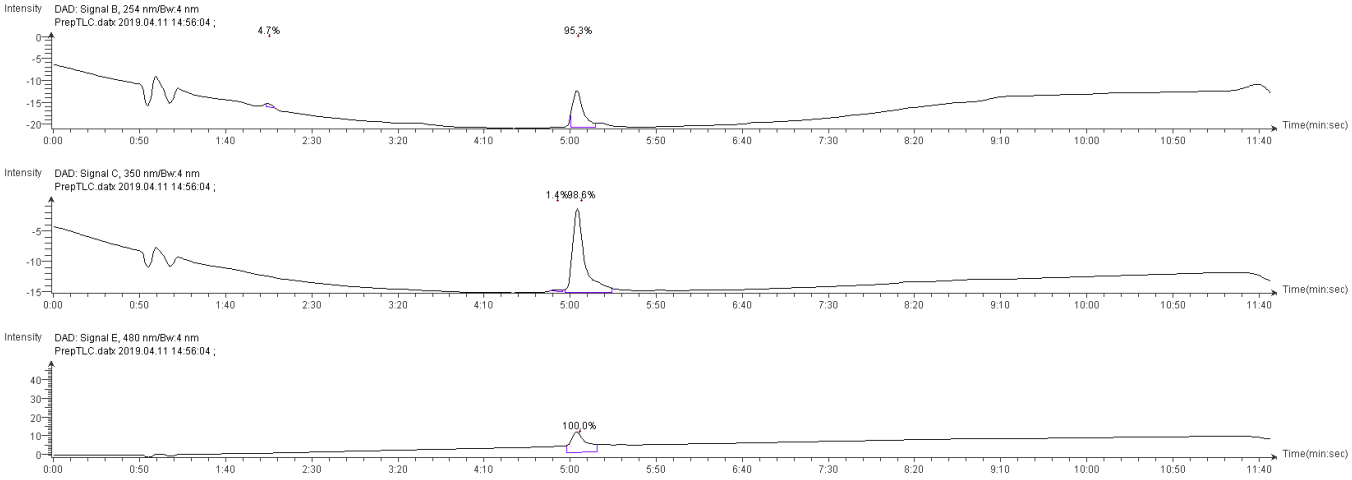

References

1 Altman, R. B. *et al.* Cyanine fluorophore derivatives with enhanced photostability. *Nature methods* **9**, 68-71, doi:10.1038/nmeth.1774 (2011).

2 Yang, Z. *et al.* Cyclooctatetraene-conjugated cyanine mitochondrial probes minimize phototoxicity in fluorescence and nanoscopic imaging. *Chemical Science* **11**, 8506-8516, doi:10.1039/D0SC02837A (2020).

3 Zheng, Q. *et al.* Ultra-stable organic fluorophores for single-molecule research. *Chemical Society Reviews* **43**, 1044-1056, doi:10.1039/C3CS60237K (2014).

4 Isselstein, M. *et al.* Self-Healing Dyes—Keeping the Promise? *The Journal of Physical Chemistry Letters* **11**, 4462-4480, doi:10.1021/acs.jpclett.9b03833 (2020).

5 Sheetz, M. P. & Koppel, D. E. Membrane damage caused by irradiation of fluorescent concanavalin A. *Proceedings of the National Academy of Sciences* **76**, 3314-3317, doi:10.1073/pnas.76.7.3314 (1979).

6 Grenier, V., Daws, B. R., Liu, P. & Miller, E. W. Spying on Neuronal Membrane Potential with Genetically Targetable Voltage Indicators. *Journal of the American Chemical Society* **141**, 1349-1358, doi:10.1021/jacs.8b11997 (2019).

7 Miller, E. W. *et al.* Optically monitoring voltage in neurons by photo-induced electron transfer through molecular wires. *Proceedings of the National Academy of Sciences* **109**, 2114-2119, doi:10.1073/pnas.1120694109 (2012).

8 Hoekstra, M., Mummery, C., Wilde, A., Bezzina, C. & Verkerk, A. Induced pluripotent stem cell derived cardiomyocytes as models for cardiac arrhythmias. *Frontiers in Physiology* **3**, doi:10.3389/fphys.2012.00346 (2012).

9 Boggess, S. C. *et al.* New Molecular Scaffolds for Fluorescent Voltage Indicators. *ACS chemical biology* **14**, 390-396, doi:10.1021/acschembio.8b00978 (2019).

10 Boggess, S. C., Gandhi, S. S., Benlian, B. R. & Miller, E. W. Vinyl-Fluorene Molecular Wires for Voltage Imaging with Enhanced Sensitivity and Reduced Phototoxicity. *J Am Chem Soc*, doi:10.1021/jacs.1c04543 (2021).